Near-ultraviolet photodetector based on hybrid polymer/zinc oxide nanorods by low-temperature solution processes

Yun-Yue Lin,[1] Chun-Wei Chen,[1,a] Wei-Che Yen,[1] Wei-Fang Su,[1] Chen-Hao Ku,[2] and Jih-Jen Wu[2]

[1]*Department of Materials Science and Engineering, National Taiwan University, Taipei 106, Taiwan*
[2]*Department of Chemical Engineering, National Cheng Kung University, Tainan 701, Taiwan*

In this article, we have proposed a nanostructured near-ultraviolet photodetector (<400 nm) based on the ZnO nanorod/polyfluorene hybrid by solution processes at low temperature. The current-voltage characteristic of the hybrid device demonstrates the typical *pn*-heterojunction diode behavior, consisting of *p*-type polymer and *n*-type ZnO nanorods, respectively. The relative quantum efficiencies of the hybrid device exhibit a nearly three order difference while illuminated under UV and visible light, respectively. The responsivity for the device can reach to 0.18 A/W at 300 nm by applying a bias of -2 V, which provides a route to fabricate a low-cost near-UV photodetector. © *2008 American Institute of Physics*. [DOI: 10.1063/1.2940594]

Due to its direct band gap of 3.37 eV and strong exciton binding energy of 60 meV, ZnO-based semiconductors are recognized as very promising photonic materials in the ultraviolet (UV) region.[1–3] It has been suggested that semiconducting nanowires or nanorods may offer additional advantages for optoelectronic device applications due to the increased junction area, enhanced polarization dependence, and improved carrier confinement in one dimension. Potential applications in many fields such as light emitting diodes,[4] field effect transistors,[5] and dye-sensitizer solar cell[6] have also attracted a great attention recently. Another important application for ZnO is the UV detection due to its wide band gap and chemical and thermal stability. Until now, UV detectors based on photoconducting layers[7] or metal-semiconductor Schottky barriers[8] from ZnO films have been commonly reported. Since *p*-type doping of ZnO has remained a challenge,[9] as a consequence, UV detectors based on ZnO homojunction or heterojunction structures are still very limited. Compared to most of ZnO nanostructures which are usually prepared in various gas methods in vacuum and high temperature,[10,11] much lower temperature deposition methods have been developed recently through solution processes.[12] In this work, we have developed the simple solution processes to fabricate a near-UV (NUV) detector based on a *pn*-heterojunction consisting of *p*-type polymer polyfluorene (PFO) and *n*-type ZnO nanorods. The device can be fabricated by preparing the ZnO nanorods in the much lower deposition temperature regime through solution and utilizing the simple spin-coating method to form the organic/inorganic hybrid thin films.

ZnO nanorods were grown in electrodeposition from aqueous solution on indium tin oxide (ITO) substrates ($15 \ \Omega/cm^2$) by a two-step electrochemical deposition method in a $0.005M$ zinc nitrate aqueous solutions at 95 °C.[13] A platinum wire was utilized as the counterelectrode. The potentials of -2.73 and -2.15 V relative to the Pt electrode were applied on the substrates for 1 and 10 min in sequence during the two-step electrochemical deposition.

Figure 1(a) shows the typical scanning electron microscope (SEM) image of single crystalline ZnO nanorods with orientation preferentially vertical to the ITO substrate. The diameter and the length of the nanorods are in the ranges of 80–100 and 450–500 nm, respectively. The polymer PFO used in this study was synthesized by using the Suzuki method,[14] with a molecular weight of 11 KDa and a PDI of 2.07. Figure 1(b) shows the chemical structure of the polymer PFO. The schematic representation of the hybrid ZnO nanorod/PFO device structure is shown in Fig. 1(c). A thin PFO layer was deposited to establish a *p*-type contact to the *n*-type ZnO nanorods by using spin coating. The polymer PFO layer acts as the hole transporting layer of the device, which has a typical hole mobility about $\sim 1.6 \times 10^{-5} \ cm^2/V \ s$.[15] The effective film thickness of the PFO layer is about 500 nm. The sample was then heated at temperature of 150 °C for 30 min to facilitate the infiltration of the polymer into the ZnO nanorod array. The device was then followed by spin coating a thin layer of poly(3,4-ethylenedioxythiophene)-poly(styrenesulfonate) (PEDOT:PSS) with an effective thickness of 50 nm before thermal evaporation of the Au top electrode. The films were then baked in a vacuum oven for 6 h at 120 °C. Vapor deposition of the Au top electrode was then carried out at pressure around 2×10^{-6} Torr. For the material
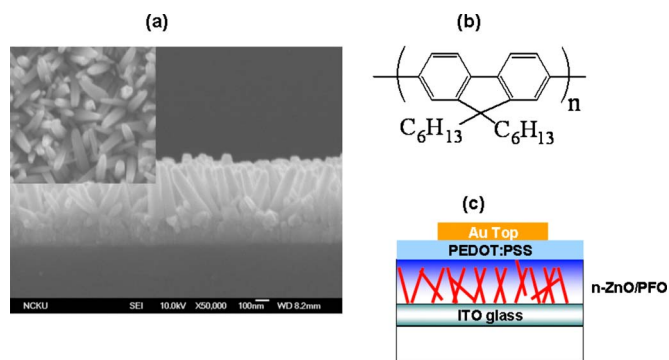
FIG. 1. (Color online) (a) The cross-sectional SEM micrograph of the ZnO nanorods. The scale bar is 100 nm. The inset shows the top view of ZnO nanorods. (b) The chemical structure of the PFO polymer. (c) Schematic diagram of the PFO/ZnO nanorod hybrid photodiode.

a)Author to whom correspondence should be addressed. Electronic mail: chunwei@ntu.edu.tw.
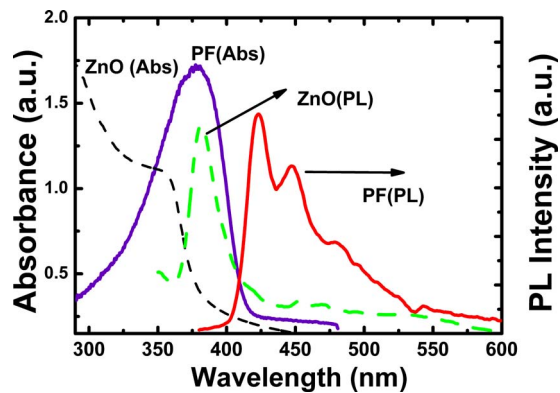
FIG. 2. (Color online) Absorption and PL spectra of ZnO nanorods (dash line) and polymer PFO (solid line) respectively.

and device characterizations, UV-visible absorption spectra were obtained using an Ocean Optics HR-4000 spectrometer. The steady-state photoluminescence (PL) spectra were measured by using a Perkin-Elmer FS-55 spectrofluorometer. Time-resolved PL (TRPL) spectroscopy was performed with a time-correlated single photon counting spectrometer (Picoquant, Inc.). A pulse laser (375 nm) with an average power of 1 mW operating at 40 MHz with a duration of 70 ps was used for excitation. The film thickness was measured by means of the Veeco M6 surface profiler. The current-voltage characterizations (Keithley 2400 source meter) were performed under 10^{-3} torr vacuum and under monochromatic illumination at defined beam size (Newport Inc.).

Figure 2(a) shows the absorption and PL spectra of the ZnO nanorods and polymer PFO used in this study. For the ZnO nanorods, the fundamental absorption edge is located in the UV region (<375 nm). The PL spectra exhibit a strong UV emission peak at about 380 nm, which is related to the near-band edge emission of the wide band gap ZnO. An additional green band at ~450–500 nm is also observed, which is mainly caused by the intrinsic defects or oxygen vacancies in the ZnO. For the polymer PFO, a broad absorption spectrum ranged from 300–400 nm with a peak at about 375 nm is observed. Since PFO has an absorption edge about 3 eV, it is also almost transparent in the visible region. In addition, the PL spectrum of PFO shows a broad emission range with two distinct vibronic peaks at 423 and 448 nm, respectively.

Figure 3(a) shows the current-voltage characteristics of the PFO/ZnO nanorod heterojunction diode measured in the dark and under illumination at 350 nm, respectively. The typical *p-n* junction behavior with the clearly rectifying current-voltage *I-V* characteristics was obtained in the dark, showing a rectification ratio (current ratio measured at +1 versus −1 V) of 122. This is originated from the formation of *p-n* junction interfaces between *p*-typed conjugated polymer and the *n*-typed ZnO nanorods. Under illumination with a 350 nm light source, a typical photovoltaic characteristic curve can be obtained, with a short circuit current density (J_{sc}) of 18 $\mu A/cm^2$, an open circuit voltage (V_{oc}) of 335 mV, a fill factor of 0.46, respectively. The dynamic range of the photodiode at zero bias (the current ratio between photocurrent and dark current) is exceeding 10^4. One of the advantages of operating a photodiode under zero or low bias voltage is the low dark current, low noise level, and large dynamic range. The relative quantum efficiencies
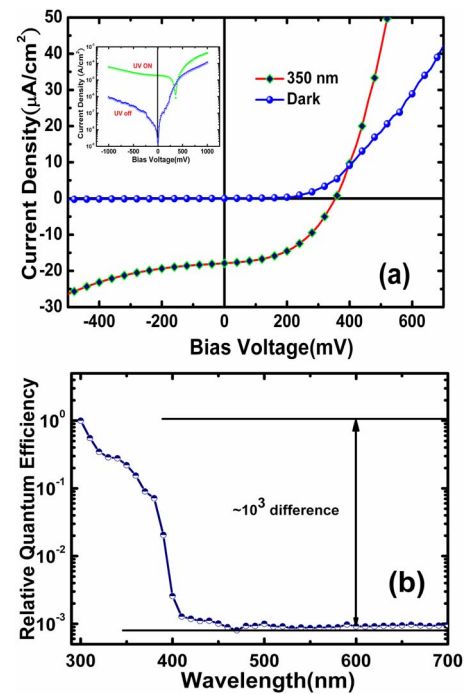
FIG. 3. (Color online) (a) Current-voltage characteristics of PFO/ZnO nanorod heterojunctions in the dark and under 350 nm illumination respectively. The incident power is 0.69 mW/cm². The inset shows the semi-log plot for the above curves. (b) The RQEs for hybrid device. The quantum efficiency under 300 nm illumination is taken as 1.

(RQEs) with a spectral range from 300 to 700 nm for the photodiode based on PFO/ZnO nanorod heterojunctions are shown in Fig. 3(b), by taking the quantum efficiency as 1 for the sample under the 300 nm illumination. The RQEs of the PFO/ZnO nanorod hybrid device exhibit a nearly three order difference while illuminated under UV (300 nm) and visible light (600 nm), respectively, indicating that the device can be used as a potentially cheap NUV photodetector fabricated from low temperature solution processes.

Figure 4(a) shows the spectral responsivity $S(\lambda)$ of the PFO/ZnO nanorod hybrid photodiode operated at different bias conditions. The number of photogenerated electron-hole pairs at the PFO/ZnO nanorod interface can be further enhanced by applying a reverse bias to the junction, which may suppress the formation of excitons or decompose excitons into mobile carriers. The responsivity can reach to about 0.18 A/W at 300 nm for the photodiode operated at −2 V reverse bias. Due to the large overlap in the UV absorption region between PFO and ZnO nanorods, the PFO thin layer can act not only as the hole transport layer but also as the light absorbing layer. The observed significant increase in $S(\lambda)$ at the wavelengths between 370 and 400 nm under −2 V bias may mainly result from the enhanced charge transfer efficiency from PFO to ZnO nanorods. The inset in the Fig. 4(b) exhibits the corresponding electronic energy levels for ZnO and PFO obtained from literatures.[16,17] When the PFO/ZnO nanorod hybrid device is illuminated with a wavelength <350 nm, both PFO and ZnO nanorods can be excited. Photogenerated excitons in ZnO or PFO can be either recombined radiatively or dissociated from Coulomb attraction at the interfaces between polymer and ZnO nanorods, by offering an energetically favorable pathway for the electrons (holes) from polymer (ZnO nanorods) to transfer onto ZnO nanorods (polymer). When the device is illumi-
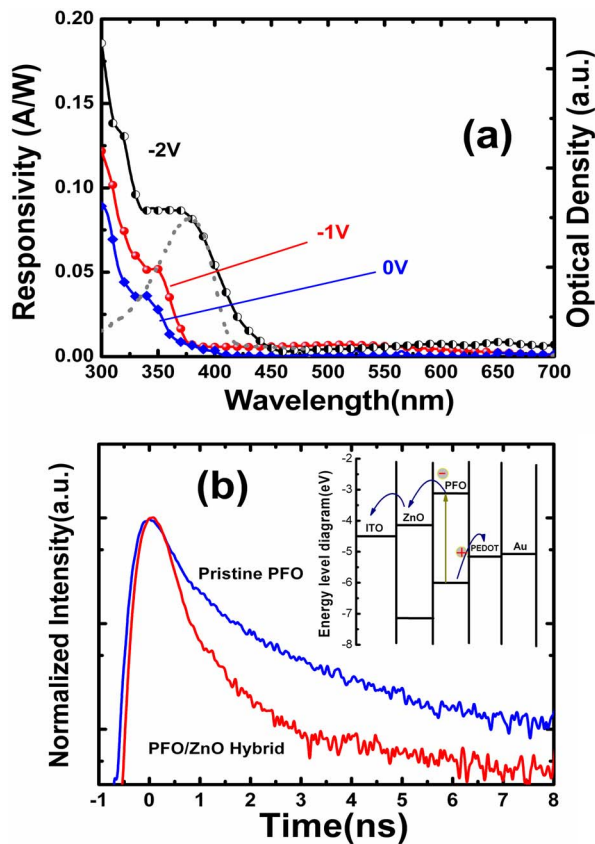
FIG. 4. (Color online) (a) Spectral response of the hybrid photodiode at different biases. The dash line shows the absorption spectra of PFO. (b) The PL decay curves for the pristine PFO and PFO/ZnO nanorod hybrid thin films, respectively. The exciting wavelength of the pulse is 375 nm and the PL emission wavelength is probed at 423 nm of PFO The inset shows the corresponding energy levels for the materials used in the device.

nated with a wavelength between 370 and 400 nm, a large number of excitons are mainly generated from polymer due to the large absorption coefficient of PFO. Figure 4(b) shows the TRPL decay spectroscopy for the pristine PFO and PFO/ZnO nanorod hybrid thin films respectively. It is found that the PL lifetime τ_{hybrid} (380 ps) for the PFO/ZnO nanorod hybrid is much shorter than that of the pristine PFO thin film

τ_{PFO} (875 ps), suggesting that charge transfer occurs from PFO to ZnO nanorods at the interfaces. This accounts for the significant increase in the photoresponse at the wavelength range between 370 and 400 nm, resulting from the efficient charge transfer from PFO to ZnO nanorods.

In conclusion, we have reported a ZnO nanorod/polymer hybrid NUV photodetector using simple low temperature solution processes. We believe this system can be a promising alternative to fabricate the low-cost NUV photodiode since the complete processes are compatible for large area and flexible substrate fabrications.

[1] H. J. Ko, Y. F. Chen, Z. Zhu, T. Yao, I. Kaobayyashi, and H. Uchiki, Appl. Phys. Lett. **76**, 1905 (2000).
[2] W. I. Park, Y. H. Jun, S. W. Jung, and G.-C. Yi, Appl. Phys. Lett. **82**, 964 (2003).
[3] M. H. Huang, S. Mao, H. Feick, H. Yan, Y. Wu, H. Kind, E. Weber, R. Russo, and P. Yang, Science **292**, 1897 (2001).
[4] A. Tsukazaki, A. Ohtomo, T. Onuma, M. Ohtani, T. Makino, M. Sumiya, K. Ohtani, S. F. Chichibu, S. Fuke, Y. Segawa, H. Ohno, H. Koinuma, and M. Kawasaki, Nat. Mater. **4**, 42 (2005).
[5] W. I. Park, J. S. Kim, G.-C. Yi, M. H. Bae, and H.-J. Lee, Appl. Phys. Lett. **85**, 5052 (2003).
[6] M. Law, L. E. Greene, J. C. Johnson, R. Saykally, and P. Yang, Nat. Mater. **4**, 455 (2005).
[7] D. Basaka, G. Aminb, B. Mallikb, G. K. Paulc, and S. K. Senc, J. Cryst. Growth **256**, 73 (2003).
[8] S. Liang, H. Sheng, Y. Liu, Z. Huo, Y. Lu, and H. Shen, J. Cryst. Growth **225**, 110 (2001).
[9] S. Limpijumnong, S. B. Zhang, S.-H. Wei, and C. H. Park, Phys. Rev. Lett. **92**, 155504 (2004).
[10] J. J. Wu, H. I. Wen, C. H. Tseng, and S. C. Liu, Adv. Funct. Mater. **14**, 806 (2004).
[11] Z. W. Pan, Z. R. Dai, and Z. L. Wang, Science **291**, 1947 (2001).
[12] C. H. Ku and J.-J. Wu, J. Phys. Chem. B **110**, 12981 (2006).
[13] J. Cui and U. J. Gibson, J. Phys. Chem. B **109**, 22074 (2005).
[14] A. Suzuki and N. Miyaura, Chem. Rev. (Washington, D.C.) **95**, 2457 (1995).
[15] R. Pacios, J. Nelson, D. C. Bradley, and C. J. Brabec, Appl. Phys. Lett. **83**, 4764 (2003).
[16] M. Graetzel, Nature (London) **414**, 338 (2001).
[17] G. Greczynskia, Th. Kugler, and W. R. Salaneck, J. Appl. Phys. **88**, 7187 (2000).